



NTNU
Norwegian University of
Science and Technology

Faculty of Engineering Science and Technology
DEPARTMENT OF PETROLEUM ENGINEERING
AND APPLIED GEOPHYSICS

Temperature profile in subsea pipelines

Effect of paraffin wax deposition on the overall
heat transfer coefficient

Håkon Eidem Christiansen

December 2011

Trondheim

Preface

Course: TPG 4510 FDP Petroleum Production Technology. This project is a preparing study in advance of the master thesis. The completion of a preparing project in the 9th semester of the Master of Technology education at the Norwegian University of Science and Technology (NTNU) is compulsory for all master students. This project is the result of work carried out from September through December 20th 2011.

The topic of this project was developed collaboration with Professor Jon Steinar Gudmundsson at the Department of Petroleum Engineering and Applied Geophysics at NTNU.

I would like to thank my supervisor Professor Jon Steinar Gudmundsson at the Department of Petroleum Engineering and Applied Geophysics at the Norwegian University of Science and Technology, for assistance and good inputs concerning the topic investigated.

Håkon Eidem Christiansen

December 20, 2011

Abstract

The temperature profile along a subsea pipeline is decided by the heat flow in the pipeline, the overall heat transfer coefficient (OHTC) of the pipeline and the ambient temperature. The temperature in the reservoir and the ambient sea temperature are uncontrollable. The OHTC depends on the pipeline materials, inside and outside fouling and insulation efforts. In this report it has been shown that paraffin wax deposition has a large effect on the OHTC of an exposed subsea pipeline. High oil content in the wax and thick deposit results in a lower OHTC, which gives less heat transfer from the hot oil to the cold sea water. Buried pipelines are insulated by the surrounding water saturated soil. And the effect on OHTC of paraffin wax deposition is small. Exposed subsea pipelines have a large potential for wax precipitating and depositing on the pipe wall. An evaluation to consider the need for pigging programs is advisable for all long distance subsea development

Table of Contents

Preface.....	ii
Abstract	iii
List of Tables.....	v
List of Figures.....	v
List of Formulas	vi
1. Introduction	1
2. Wax	2
3. Temperature profile.....	4
4. Thermal Conductivity Model	6
5. Parameters and equations.....	8
6. Calculations.....	11
7. Discussion.....	14
8. Conclusion.....	16
9. Nomenclature	17
10. References.....	19
11. Tables	22
12. Figures	24
13. Formulas.....	30
14. Appendices	32
14.1 Re-writing to Maxwell-Eucken.....	32
14.2 Calculation data references.....	33
14.3 Calculation procedure	33
14.4 Details on numerical model.....	39

List of Tables

TABLE 1: CALCULATION DATA.....	22
TABLE 2: TEMPERATURE PROFILE CASES.	23
TABLE 3: TYPICAL COMPOSITIONS OF PETROLEUM RESERVOIR FLUIDS. (GUDMUNDSSON, PRODUCED AND PROCESSED NATURGASS, 2011).....	23
TABLE 4: CALCULATED VALUES FOR DEPOSIT CONDUCTIVITY, FLOW PARAMETERS AND DIMENSIONLESS PARAMETERS FOR CONDUCTION AND HEAT RESISTANCE/HEAT TRANSFER COEFFICIENT IN THE LAMINAR SUB-LAYER AND ON THE PIPELINE'S OUTSIDE.	34
TABLE 5: TEMPERATURE PROFILE TABLE	35

List of Figures

FIGURE 1: THE CLOUD POINT AND POUR POINT OF REFINED OIL WITH DIFFERENT WAX CONCENTRATIONS. (GUDMUNDSSON, PIPELINE FLOW ASSURANCE, 2010).....	24
FIGURE 2: SHOWS THE DISTRIBUTION AND THE RANGE OF HYDROCARBONS FOUND IN PARAFFIN WAX (GUDMUNDSSON, PIPELINE FLOW ASSURANCE, 2010).....	24
FIGURE 3: WAX DEPOSIT BUILDING UP WITH TIME UNTIL THERE IS NO ACTIVE TEMPERATURE DRIVING FORCE (GUDMUNDSSON, PIPELINE FLOW ASSURANCE, 2010).	25
FIGURE 4: WAX DEPOSITS BUILDING UP AND MOVING DOWN THE PIPELINE WITH TIME (GUDMUNDSSON, PIPELINE FLOW ASSURANCE, 2010).	25
FIGURE 5: 3D-NETWORK OF WAX CONTAINING PORES WITH OIL (BURGER, ET AL., 1981).....	26
FIGURE 6: CROSS-SECTIONAL TEMPERATURE PROFILE IN A SUBSEA PIPELINE (ROSVOLD, 2008).	26
FIGURE 7: TWO PHASE THERMAL CONDUCT MODEL. THREE SAMPLES OF DIFFERENT DISTRIBUTION OF ONE MEDIUM IN ANOTHER MEDIUM (TANG, ET AL., 2009).....	27
FIGURE 8: THEORETICAL THERMAL CONDUCTIVITY MODELS FOR DISCONTINUOUS TWO PHASE DISTRIBUTION (TANG, ET AL., 2009).	27
FIGURE 9: THEORETICAL AND NUMERICAL OBTAINED EFFECTIVE THERMAL CONDUCTIVITIES OVER A RANGE OF V_2 FOR TWO PHASE MIXTURES.....	28
FIGURE 10: OHTC FOR SELECTED WAX THICKNESSES DIVIDED BY OHTC FOR A CLEAN PIPE, WITH DIFFERENT OF LIQUID VOLUME %.	28
FIGURE 11: WAX DEPOSIT THICKNESS VS. U	29
FIGURE 12: SUBSEA PIPELINE TEMPERATURE PROFILE. HORIZONTAL LINES ARE CLOUD POINT, POUR POINT AND AMBIENT TEMPERATURE FROM TOP TO BOTTOM.....	29
FIGURE 13: NUMERICAL MODEL (TANG, ET AL., 2009).....	40

List of Formulas

FORMULA 1: MAXWELL-EUCKEN MODEL FOR EFFECTIVE THERMAL CONDUCTIVITY IN WAX DEPOSITS. 30

FORMULA 2: NUSSELT NUMBER. 30

FORMULA 3: REYNOLDS NUMBER. 30

FORMULA 4: PRANDTL NUMBER. 30

FORMULA 5: DIMENSIONLESS RELATIONSHIP FOR PIPE FLOW (GUDMUNDSSON, 2010)..... 30

FORMULA 6: THE CHURCHILL-BERSTEIN EQUATION (MEHROTRA, ET AL., 2004)..... 30

FORMULA 7: OVERALL HEAT TRANSFER COEFFICIENT FOR A SUBSEA PIPELINE. 30

FORMULA 8: OVERALL HEAT TRANSFER COEFFICIENT FOR A COMPLETELY BURIED SUBSEA PIPELINE (LOCH,
2000). 31

FORMULA 9: HEAT TRANSFER COEFFICIENT FOR PARTLY BURIED PIPE (BAI & BAI, 2010). 31

FORMULA 10: THE BULK TEMPERATURE IN STEADY-STATE PIPELINE FLOW WITH CONSTANT AMBIENT
TEMPERATURE (GUDMUNDSSON, 2010). 31

FORMULA 12: HEAT TRANSFER RESISTANCE FOR PIPE LAYER N..... 31

FORMULA 13: HEAT TRANSFER RESISTANCE IN SOIL 31

FORMULA 11: RE-WRITING TO THE FORM OF MAXWELL-EUCKEN MODEL. $A = V_2$ 32

1. Introduction

When oil and gas is cooled inside a pipeline a number of problems can appear. The temperature drop decreases the solubility of the components and paraffin wax precipitate and water condensate. The water molecules can form hydrates with small hydrocarbon molecules and precipitated wax may deposit on the pipe wall. This can lead to lower flow rate, higher pressure loss and/or clogging of the pipeline.

Decreased flow rate results in lower production of hydrocarbons and thereby lower revenue. Higher pressure loss may lead to a shorter plateau production or earlier need for pressure support of the reservoir. Clogging of the pipeline may lead to an expensive removal of a pipeline section, the abandonment of a pipeline, the abandonment of a field, or a potential environmental disaster if the pipeline should burst/leak.

A lot of papers have been written on the subject of wax deposition models to find out where and when deposits may build up. With this information the oil companies can plan a pigging program to prevent the deposits to build up to a critical level. The pigs can get stuck in the pipeline if they are launched too seldom, or are improperly constructed.

In this project I have tried to identify the parameters that affect the temperature profile along a subsea pipeline. And my focus has been on how paraffin wax deposits on the pipe wall will affect the total heat transfer coefficient of the subsea pipeline. The results will be used to identify if a pipeline has the potential of wax deposition and to say something about the pigging frequency of pipelines which suffers from wax deposition.

2. Wax

Oil and gas flows from the reservoir, up the well and then either to an offshore processing plant (platform) or an onshore process facility through subsea pipelines. In this transportation process the fluids cool slightly down from reservoir temperature up to the well head because of the insulation provided by the surrounding warm rock. But when it enters the subsea pipeline it is exposed cooling from the ambient temperature of sea water of approximately four degrees Celsius.

The cooling of the fluids gives room to a number of issues which can be solved by flow assurance. The problem discussed in this paper is paraffin wax deposition. There are several ways to stop these problems from occurring; injecting chemicals, injecting inhibitor, insulation or heating of the pipeline. But these measures are expensive, and for long distance transportation they are often not an option because of the costs.

Paraffin wax precipitation is highly dependent on the temperature of the oil. Wax crystal starts to form and precipitate when the temperature sinks to wax appearing temperature (WAT). A typical WAT can be around 40 °C. The WAT is also called the cloud point, and further cooling will cause the wax gel to stop flowing. When this happens the temperature has reached the pour point, typically 15 degrees Celsius below the cloud point. "Pure paraffin wax is solid at ambient temperatures" (Gudmundsson, 2010). A WAT and pour point plot is exposed in Figure 1.

Wax is a common constituent of both oil and condensate. Typical wax content is in the range from 1-15 weight % (Ask, 2007). The wax crystals consist mostly of straight-chain alkanes in the range C₁₈-C₄₀, and their general chemical formula is C₂H_{2n+2}. The hydrocarbons in the wax are normal distributed between n=20 and n=40 with some skewness. Typical distributions of wax alkanes are shown in Figure 2.

When the wax crystals deposit on the pipe wall they form an insulating layer which reduces the heat transfer between the hot oil and the ambient sea water. The layer will get thicker with time until there is no active temperature driving force (Figure 3). When the deposition

of paraffin wax is halting at the first location, the precipitated wax crystals will deposit further down the pipeline where the temperature driving force is larger. As this is a transient procedure the deposition will move down the pipeline with time (Figure 4).

The precipitated wax crystals enclose oil when they deposit on the pipe wall. It is widely believed that the deposit forms a network of wax solids with pores of oil separated from another (Figure 5) (Burger, et al., 1981). The oil content can be as high as 90 %, but Statoil uses 60 % as base case (Rosvold, 2008). How much oil is enclosed depends on how fast the wax crystals are cooled. Fast cooling leads to a soft mush with high oil content, and slower cooling can lead to harder deposit with less oil content. The latter case is more likely in subsea pipelines because turbulent flow is such a good heat transmitter.

With time the oil content in the incipient wax film is reduced and the wax deposit hardens. This is a result of a counter-diffusion phenomenon, where wax molecules diffuse into the wax gel and oil diffuse out. The thickness and wax content of the deposit is found to be a function of the flow rate in the pipe. (Singh, et al., 2000)

Pipelines with wax deposition have to be cleaned from time to time to avoid large deposits of wax building up. A common method is called pigging. It is a mechanical removal of deposited wax. A pig can vary in shape and size, from very simple designs to more advanced. If the wax deposit is too thick or too hard the pig might get stuck in the pipeline, and serious problem can arise.

The frequency of the pig launches vary from pipeline to pipeline. It is among other things dependent on the wax deposition rate, the pipe diameter and the pipeline length. For some crude oil transportation pipelines in the Gulf of Mexico pigs have to be launched every 3-5 days (O'Donoghue, 2004).

The deposition growth with time can be estimated using deposition models. An asymptotic development of the deposition thickness will occur when deposition driving force depends on heat transfer at the wall. The deposition-release model provides good results for a range of deposition situations. (Gudmundsson, 2010)

3. Temperature profile

Reservoir temperature is high due to the thermal gradient in the earth's crust. Temperatures can be well above 100 degrees Celsius. When the oil is produced from a well it does not lose much of its heat on its way to the sea bottom because the well is surrounded by hot rock. Many wells are located far from platforms, and crude oil often has to be transported over long distances in subsea pipelines. The oil is cooled on its way to the destination due to heat transfer, through the pipelines walls, with the surrounding sea water. And temperature related transportation problems can take place.

The radial heat transfer between the flowing oil and the ambient seawater is induced by their temperature. If the pipelines is not insulated the temperature will drop quickly. This may lead to the precipitation of asphaltenes and/or paraffin wax and the formation of hydrates. These flow assurance problems can result in lost production and blocking of the pipelines.

For steady state conditions the heat effect through each heat resistance layer is constant. The size of the temperature drop is dependent on the layer's heat transfer coefficient. The heat transfer coefficient from the bulk flow to the wall is decided by the sub-layer coefficient. Hence temperature drop across each layer is constant, and decided by the material's heat conduction properties and thickness. On the outside of the pipe wall heat is transferred either through water saturated mud/soil, or by a cross-flow of a subsea current (Figure 6).

Then heat is conducted through the different materials that make up the pipelines. Every material has different heat transfer properties. Steel is a good heat conductor, while concrete is not. Most of the heat loss in a subsea pipeline is found to happen outside of the steel pipe (Gudmundsson, 2010). Small heat transfer resistance gives a small temperature drop and a fast cooling process, which is not wanted.

For fully developed turbulent flow in a pipeline the turbulent eddies effective in transferring heat radial to the pipe wall. Only significant heat transfer resistance is in the viscous sub-

layer. In turbulent flow there is a thin laminar layer on the pipe wall where the heat transfer is mainly due to conduction. At the wall the speed is zero, but increases linearly until the end of the viscous sub-layer. Its thickness increases with larger viscosity and decreases with increasing average speed and density of the fluid (Gudmundsson, 2010).

Even in the simplest subsea pipelines there is a layer of re-enforced concrete on the outside of the steel pipe to prevent floating. In addition, the pipeline may be buried, insulated, heated or it could be exposed to deposited paraffin wax. All these factors will contribute to smaller heat loss, and affect the overall heat transfer coefficient (OHTC) of the pipeline. Experimental data shows that insulated pipelines have an OHTC of approximately $2 \text{ W/m}^2\text{K}$, and bare pipelines approximately $20 \text{ W/m}^2\text{K}$ (Gudmundsson, 2011).

To insulate a subsea pipeline a passive or active strategy can be chosen. Most used for longer transportation is passive strategy. Three common technologies are; external coatings, pipeline burial or Pipe-in-Pipe (PIP). Active strategies can be direct electrical heating or hot water annulus. All the strategies are effective, but also very costly (Bai & Bai, 2010).

4. Thermal Conductivity Model

My task was to show how much the deposition of wax in a subsea pipeline could affect the temperature profile. The idea was to calculate how the overall thermal conductivity coefficient, U , was changing when paraffin wax was deposited on the pipeline wall. In order to be able to account for the deposition of wax, I had to find the proper way to calculate the effective conductivity of the wax-mixture.

The wax-mixture deposited on a pipeline wall contains oil. How much oil it contains is a function of the precipitation drive forces and the speed of the flow, also known as the aging of the wax. But it may contain up to 90 % oil allocated as a discontinuous medium within the wax layer, and resemble a simple granular medium.

To solve this problem a search for methods of calculating the effective thermal conductivity in papers and books had to be conducted. There are different models for different distributions of a medium with dissimilar thermal conductivity within another medium. These models are often based on existing scientific principles, or by adapting equations to experimental results.

Different distributions, serial sample, parallel sample and disordered sample, are shown in Figure 7. The flux-arrow indicates which direction the heat is conducted through the solid. V and λ are respectively volume and thermal conductivity of medium one and two. Figure 5 shows the structure of a wax deposit, and the distribution of oil in wax resembles the disordered sample (Sp#3) in Figure 7.

Comparison of a detailed numerical model and the theoretical model; Maxwell-Hamilton and Woodside-Messmer (Figure 8), is shown in Figure 9. The test shows similar values for the effective thermal conductivity in Sp#3 (Tang, et al., 2009). Both theoretical models are functions of the volume of the discontinuous phase. Details on the numerical model used by (Tang, et al., 2009) for comparison can be found in the appendix.

Certain models are often used, and one in particular: The Maxwell-Hamilton model. The model "is mathematically the same as induced magnetization in a body if the same shape

placed in a uniform external field, and solutions will be found on the text books on electricity and magnetism” (Carlslaw, et al., 1959). The Maxwell-Hamilton uses the exact results of the ellipsoidal and spherical model as a statistically tool to predict the thermal conductivity of medium distributed in another medium. The model regards the discontinuous medium as a number of spherical particles of the same material distributed in the continuous medium.

It is widely accepted that paraffin wax depositions are considered as a porous medium with oil trapped inside the crystalline structure (Burger, et al., 1981). The classical model for predicting the thermal conductivity of a porous medium consisting of a continuous phase and a discontinuous phase is the Maxwell-Eucken model (Formula 1).

The Maxwell-Eucken model builds on the more general Maxwell-Hamilton model. When the phase distribution coefficient, n equals three, the Maxwell-Hamilton is applicable to any system consisting of continuous and discontinuous phase. Numerous examples of its use are found in the literature (Singh, et al., 2000). The Maxwell-Eucken model is based on a statistical distribution of a number of spheres of the same material, where “the spheres are so far apart that they have no influence on one another”.

5. Parameters and equations

The prime goal of this paper was to look at how deposited paraffin wax on the pipe wall would affect the total heat transfer coefficient. This made it essential to find a suitable model for calculating the effective thermal conductivity for wax deposits. The literature indicated that the deposit was build up of continuous phase of wax and a discontinuous phase of oil. This meant the deposit could be looked at as a porous medium with a discontinuous phase. And the thermal conductivity could be calculated by the use of the Maxwell-Eucken model (Formula 1).

The heat transfer coefficient of oil describes how well heat is transferred from the oil to the wall. It is difficult to estimate because it depends on many factors. Among other are: The wall's geometry, material, flow conditions, temperature difference between pipe wall and fluid and the fluid properties. That is why we use semi-empirical correlations with dimensionless numbers to calculate the heat transfer coefficient.

In my calculations the dimensionless numbers that were used was: The Nusselt number (Formula 2), Reynolds number (Formula 3) and the Prandtl number (Formula 4). At steady state conditions the Nusselt number can be expressed as a function dependent on Re , Pr and Gr . In pipe flow where only forced convection is contributing to the heat transfer we disregard Gr , and the Nusselt function is reduced to the classical relationship for pipe flow: Formula 5.

The heat transfer coefficient for the pipe's outside is dependent on the fluid and flow properties of the sea. A current with a velocity of 0,1 m/s is assumed. The same dimensionless equations are used, just with water properties. But the Nusselt number can now be expressed with Formula 6. The outside fouling resistance is caused by a layer of water saturated mud. And deposits like wax contribute to the inside fouling resistance.

The overall heat transfer coefficient (OHTC), with respect to the inside area of the pipeline, can be calculated using the overall heat transfer coefficient equation for thick walled pipes. The equation is based on Fourier's equation for heat transfer through parallel layers. The

sum of the heat transfer resistance, which is the inverse of U, determines the total resistance. On general form Formula 7, and adapted for buried pipes Formula 8.

The summation part accounts for the heat resistance in the different materials that makes up the pipeline, that is, the steel pipe and the concrete anti-float. R_{fi} and R_{fu} is the fouling resistance on the inside and outside of the pipe, namely, wax deposition on the inside and water saturated mud on the outside. h_i and h_u refers to the inside and outside heat transfer area respectively. That is, the heat coefficient in the laminar sub layer inside the pipe and the heat transfer coefficient from a subsea current.

ID/OD (inside and outside diameter) is a correction term because the equation is referenced to inside pipe diameter. And the last term in Formula 8 is included to model a completely buried pipe line, where H is the depth of the center of the pipeline. Completely buried pipeline implies that H is larger than OD/2. The thermal conductivity of water saturated soil approaches the value of still sea water for wet soil.

The theoretical assumption for the exposed pipe is that the water flows both beneath the bottom and over the top of the pipe. In the case of a fully buried pipe the soil heats up around the pipe and acts like an insulating pipe layer. A partly buried pipe can be modeled by the simple relationship in Formula 9. f is the fraction of the outside surface of the pipe exposed to the surrounding fluid (Bai & Bai, 2010). $h_{exposed}$ are calculated from the Churchill-Bernstein equation, and h_{soil} is the inverse of Formula 12.

For my case the only heat transfer resistances that are varying are the inside and the outside fouling resistance. As mentioned above they are dependent on deposits on the inside and outside of the pipe, like paraffin wax and water saturated mud. These layers are thin which leads to the assumption that their inside surface area is equal to the outside surface area and does not need to be radius corrected. The other resistances are constant and calculated from flow conditions, fluid properties, pipe geometry found in the literature, calculated in HYSYS or assumed.

Temperature profiles for steady state flow in subsea pipelines can be estimated with Formula 10. With a value for the inlet temperature and a constant ambient temperature it can be used to estimate the bulk flow temperature at any distance from the inlet (wellhead). The OHTC is the most important factor in the temperature profile development. Large OHTC will cause the temperature to drop rapidly towards ambient temperature.

6. Calculations

These calculations were made to illustrate the effect on the temperature profile of wax deposits in pipelines. Wax crystals formed when exposed to a low temperature gradient will have a large content of oil. Due to aging the deposit will get harder with time, and thus a less effective insulator. While the wax is aging it also becomes more difficult to remove with pigs. Information about the calculation data in Table 1 can be found in

Calculation data references in the appendix. A detailed procedure for my calculations is also provided in the appendix.

To find values for the volatile oil I entered its composition into HYSYS, together with pressure, temperature and calculated volume flow rate. The values of the heat capacity, viscosity and density I found at inlet pressure and temperature (70 °C and 70 bar). I found the oil's thermal conductivity at WAT. k_{oil} was found to be 0,0944 [W/mK], which is close to the value in the appendix to Solids in Oil and Gas Transport ($k_{oil}=0,1$ [W/mK]) (Gudmundsson, 2010).

By using typical data for pipeline flow (Table 1). I calculated OHTC for buried and un-buried subsea pipelines with and without wax deposits (Formula 7 and Formula 8). I made calculations for a clean pipe and for different wax deposit thicknesses with different levels of aging. The wax deposits were assumed to be uniformly distributed throughout the whole pipeline, and the pipeline is covered by a 1.5 cm thick layer of water saturated mud. A subsea current with the velocity of 0.1 [m/s] is contributing to the cooling.

The data used is meant to resemble a tie-back of a satellite field/well to an existing infrastructure. It can also be applied to a smaller pipeline, transporting volatile oil to a tie-in for further transport. Inlet temperature is a typical wellhead temperature for wells in the North Sea. The volatile oil's composition is shown in Table 3.

I made a plot where I looked at the effect of deposition thickness and oil entrainment on OHTC. How oil entrainment in the paraffin wax affects OHTC as well as the deposition thickness is shown in Figure 10. This is expected because more oil in the wax deposit results in lower heat conductivity since oil is a worse heat transmitter than pure paraffin wax.

The development of OHTC with increasing deposition thickness is shown in Figure 11. To illustrate the effect of oil entrainment I have included a layer of pure wax. This plot shows the same results as the one above. More liquid oil entrained in the wax deposit has a stronger insulating effect. For buried pipelines wax deposit has little effect on OHTC.

After acquiring the value of OHTC for different flow conditions I made a plot of how the temperature in the pipe was developing with distance from the inlet. In my case a pipeline is transporting volatile oil from a well head/cluster to a processing plant/platform. Figure 12

shows the temperature development over a distance of 20 km. The assumption of a WAT of 40 °C and a corresponding pour point of 25 °C is taken from Gudmundsson's compendium; Solids in Oil and Gas production. The WAT, the pour point and ambient sea water are marked with black lines in the plot.

I have chosen to look at seven cases with different OHTC. Case one: Un-buried pipe with clean walls. Case two: Pipe buried beneath 30 cm soil with clean walls. Case three: Un-buried pipe with 5mm thick wax deposit and 30% oil. Case four: Un-buried pipe with 5mm thick wax deposit and 90% oil. Case five: Un-buried pipe with 10mm thick wax deposit and 30% oil. Case six: Un-buried pipe with 10 mm thick wax deposit and 60% oil. Case seven: Un-buried pipe with 10mm thick wax deposit and 90% oil (Table 2).

The bulk temperature drops quickly for the un-buried clean pipe. And we will start to get precipitated wax in the pipeline after only 5.4 km. In fact it will happen even earlier because the pipe wall temperature is a couple of degrees lower than the bulk temperature. For case three we will get precipitated paraffin wax crystals after 8.1 km.

For case four and five WAT is reached after 10.4- and 10.9 km. Even though case four has twice as thick wax deposit there is not much difference in OHTC. That is because of the difference in oil entrainment in the two cases. In case six WAT is reached after 12.7 km, and in case seven WAT is reached after 15.7 km. For the buried pipelines the OHTC is low because the soil is insulating the pipelines and there is only a small temperature drop.

For case one and three the oil is cooled below the pour point before it reaches its destination. The wax saturated oil gel will no longer be able to flow (Gudmundsson, 2010) and may cause major problems for the operation of the pipelines.

In the appendix of Gudmundsson's Flow Assurance, Solids in Oil and Gas Production, it has been shown that in a steel pipe most of the temperature drop is across the material outside of the steel pipe wall. Even with a concrete layer it does not change the conclusion. But the buildup of a wax deposit on the inside pipe wall may affect it considerably.

The result of the calculations shows the insulating effect of the paraffin wax layer with different thickness and different oil content. As expected the fouling resistance will increase

with deposition thickness and oil content. A local temperature increase where the wax is depositing may be measured.

Paraffin wax deposition reduces OHTC in the pipeline where it builds up. This results in slower cooling of the flowing oil. This may lead to a higher outlet temperature than expected. If the flow rate and the inlet temperature are known one can estimate the outlet temperature based on the pipeline's OHTC. By monitoring the real outlet temperature deviations from expected value may be identified. If a temperature increase is observed it could be the result of inside fouling like wax deposition.

7. Discussion

It is shown that it is unrealistic to expect that a model that is depended on component conductivity and volume fraction alone to provide accurate solutions for all porous materials (Carsona, et al., 2003). And that the effective thermal conductivity is much more affected by the contact between the particles or pores compared to the shape and size of these particles or pores.

The wax deposit structure is a 3D-network of fluid pores separated by a solid wax structure. In terms of heat conduction it can be modeled as a porous medium filled with liquid. Both the theoretical models mentioned (Figure 8), showed approximately the same results as the numerical model. But the Maxwell-Eucken model seems to be more widely used in the literature, and it is more related to fundamental science.

My calculations are based on typical pipeline data with single phase flow and uniformly distributed wax deposits in the pipeline. They show a large effect on OHTC for the un-buried pipeline. The results are meant to illustrate the effect of wax deposits on OHTC. Even though the exact results cannot be transferred to another pipeline system with another transportation fluid, they do indicate that inside fouling can greatly affect the OHTC.

For comparison I chose to look at a pipeline buried in sediments on the sea floor. The OHTC is much lower due to the insulating effect of the surrounding water saturated soil. The pipeline is no longer exposed to the cooling sea current, and the sediments heats up with time. Calculated results shows values close to those for insulated pipelines (Bai & Bai, 2010).

The wax deposit has a large effect on OHTC for the un-buried pipeline in my study. A 10 mm thick layer of wax reduces the OHTC by 50% and WAT is reached 13 km down the line. This is for a very conservative assumption of only 30% oil in the wax deposit. Statoil uses 60 % as a base case, and for case six the WAT is reached after 15.1 km.

Paraffin wax can deposit not only from heavy crudes, but also from volatile oils and condensate. For the case of exposed pipe studied in this project there is a large potential for wax deposition because of the high OHTC. For larger transport distances the temperature

will drop towards ambient temperature. To avoid serious problems due to wax deposition it would be advisable to investigate the wax content of the hydrocarbon fluid and the properties of the wax before full scale production.

A temperature profile for a clean pipe could be made with knowledge of the OHTC. With the use of the boundary layer temperature profile the corresponding wall temperature can also be estimated. These results may then be used to find out where in the pipeline wax crystals would start to precipitate, assumed known WAT. The wax deposition growth rate can be estimated by the use of deposition models. And the frequency of pigging could be planned on this information. The rate of pig launches depends on the deposition rate and the rate of aging.

By monitoring the pipeline's outlet temperature one can identify deviations that may indicate inside fouling like wax deposition if the inlet flow rate and temperature is known. For real a case the wax deposition cannot be assumed uniformly distributed throughout the pipeline. This makes it hard to know if the deposit is thick and short, or thinner and longer.

The pipeline's outlet temperature may be used to calculate an average OHTC. It can again be used to calculate the deposition thickness and volume if we assume uniformly distributed wax deposition in the pipeline. The knowledge of the amount of deposited paraffin wax may be used to plan the pigging frequency.

Another method may be to use intelligent pigs to measure the thickness and extent of the wax deposit on different occasions. This information can be related to the outlet temperature to make a model for the pipeline. The model may provide more accurate information to base the pigging frequency on.

8. Conclusion

The thermal conductivity of the paraffin wax deposit has to be between the one's for pure paraffin wax and oil. The Maxwell-Eucken model is widely used in the literature and is based on fundamental science. That is why it is the chosen model in this report.

Both the oil content in the paraffin wax and its thickness has a large effect on the overall heat transfer coefficient for exposed subsea pipelines. Increasing amount of both reduces the OHTC and thus decreasing the cooling rate of the pipe flow.

The exposed subsea pipeline has the potential of wax deposition when the transport distance exceeds 5.4 km. If the volatile oil has a large wax weight% there is a risk of wax depositing which deteriorates the production.

Wax deposition has less effect on the OHTC when it has a low value, as in the case of the buried pipeline.

Estimations of total wax volume in the pipeline can be made by monitoring the outlet temperature when the inlet flow rate and temperature is known. This information may be used to plan pigging frequency.

9. Nomenclature

Symbol	Explanation	Unit
ρ	Density	[kg/m ³]
μ	Viscosity	[Pas]
C_p	Heat capacity	[J/kgK]
d	Diameter	[m]
ID	Inner diameter	[m]
OD	Outer diameter	[m]
f	Fraction of pipe surface exposed to cooling sea current	
h_i	Inside heat transfer coefficient	[W/m ² K]
h_o	Outside heat transfer coefficient	[W/m ² K]
h	Heat transfer coefficient	[W/m ² K]
H	Distance from buried pipe center to seabed. $H > OD/2$	[m]
k_{soil}	Thermal conductivity of water saturated soil	[W/mK]
k	Thermal conductivity	[W/mK]
k_n	Thermal conductivity of layer n	[W/mK]
L	Distance from inlet	[m]

m	Mass rate	[kg/s]
Nu	Nusselt number	
Pr	Prandtl number	
Re	Reynolds number	
R_{fi}	Inside fouling resistance	[m ² K/W]
R_{fu}	Outside fouling resistance	[m ² K/W]
T_2	Temperature at distance L	[°C]
T_a	Ambient temperature	[°C]
T_{inlet}	Inlet temperature	[°C]
U	Overall heat transfer coefficient (OHTC)	[W/m ² K]
u	Average velocity	[m/s]
V_{oil}	Volume fraction of oil in wax deposit.	

10. References

- Ask Narve Wax - A Flow Assurance Challenge** [Online] // Jon Steinar Gudmundsson Hjemmeside. - 2007. -
<http://www.ipt.ntnu.no/~jsg/undervisning/prosessering/gjester/LysarkAske2007.pdf>.
- Bacon M.M., Romero-Zerón L.B and Chong K.K.** Using Cross-Polarized Microscopy to Optimize Wax-Treatment Methods [Conference] // SPE Annual Conference and Exhibition. - New Orleans : [s.n.], 4-7 October.
- Bai Yong og Bai Qiang** Subsea Engineering Handbook [Del av bok]. - [s.l.] : Gulf Professional Publishing, 2010.
- Burger E.D., ARCO Oil and Gas Co., Perkins T.K., ARCO Oil and Gas Co. and Striegler J.H., ARCO Oil and Gas Co** Studies of Wax Deposition in the Trans Alaska Pipeline [Online] // www.onepetro.org. - June 1981. -
<http://www.onepetro.org/mslib/servlet/onepetropreview?id=00008788&soc=SPE>.
- Carlslaw H.S. og Jaeger J.C.** Conduction of Heat in Solids [Del av bok] // Conduction of Heat in Solids / bokforf. H.S. Carlslaw. og Jaeger J.C.. - USA : Oxford University Press, 1959.
- Carsona J.K. [et al.]** An analysis of the influence of material structure on the effective thermal conductivity of theoretical porous materials using finite element simulations. - June 4, 2003.
- Gudmundsson Jon Steinar** 6. Varmeovergang og varmevekslere [Del av bok] // Prosessering av Petroleum; Grunnleggende enhetsoperasjoner i produksjon av olje og gass. - Trondheim : NTNU, 2009.
- Gudmundsson Jon Steinar** Pipeline Flow Assurance [Online] // www.ipt.ntnu.no/jsg. - 2010. -
<http://www.ipt.ntnu.no/~jsg/undervisning/naturgass/lysark/LysarkGudmundssonPipelineFlowAssurance2010.pdf>.

Gudmundsson Jon Steinar Produced and Processed Natural Gas [Internett] // <http://www.ipt.ntnu.no/~jsg/undervisning/naturgass/TPG4140.html>. - 29 September 2011. - <http://www.ipt.ntnu.no/~jsg/undervisning/naturgass/lysark/LysarkGudmundssonProducedProcessed2010.pdf>.

Gudmundsson Jon Steinar Solids in Oil and Gas Production [Book Section] // Solids in Oil and Gas Production. - Trondheim : [s.n.], 2010.

Gudmundsson Jon Steinar Solids in Oil and Gas Production [Book Section] // Solids in Oil and Gas Production. - Trondheim : [s.n.], 2010.

Gudmundsson Jon Steinar Solids in Oil and Gas Production [Del av bok]. - Trondheim : NTNU, 2010.

Gudmundsson Jon Steinar Specialization Project 2011, Håkon Eidem Christiansen [Rapport]. - Trondheim : Jon Steinar Gudmundsson, 2011.

Loch Kenneth [Internett] // www.worldoil.com. - 2000. - <http://www.worldoil.com/August-2000-Deepwater-soil-thermally-insulates-buried-flowlines.html>.

Mehrotra Anil K. and Bidmus Hamid O. Heat-Transfer Calculations for Predicting Solids Deposition in Pipeline Transportation of “Waxy” Crude Oils [Online] // http://www.accessengineeringlibrary.com/mghpdf/0071475192_ar025.pdf. - 2004. - http://www.accessengineeringlibrary.com/mghpdf/0071475192_ar025.pdf.

O'Donoghue Aidan Pigging as a Flow Assurance Solution – Estimating Pigging Frequency for Dewaxing [Internett] // <http://www.pipeline-research.com>. - 2004. - <http://www.pipeline-research.com/Dewax%20Frequency.pdf>.

Rosvold Karianne Wax Deposition Models [Report]. - Trondheim : NTNU, 2008.

Singh Probjot, Venkatesan Ramachandran and Fogler and H. Scott Formation and Aging of Incipient Thin Film [Journal] // AIChE Journal. - [s.l.] : AIChE Journal, 2000. - pp. 1059-1074.

Tang S.B. [et al.] Numerical Investigation of Effective Thermal Conductivity of Rock-like Material Using Mesoscopic Method. - 2009.

Toolbox The Engineering The Engineering Toolbox [Internett] // The Engineering Toolbox. -
http://www.engineeringtoolbox.com/thermal-conductivity-d_429.html.

11. Tables

Table 1: Calculation data

Data		
Physical properties	Value	Unit
Pipe properties:		
Wall thickness	0,0120	[m]
Inner diameter	0,3048	[m]
Outer diameter	0,3288	[m]
Total Pipe diameter	0,3796	[m]
Flow Area	0,0730	[m ²]
Concrete thickness	0,0254	[m]
Length	2E+04	[m]
Thermal conductivity:		
Wax:	0,25	[W/mK]
Oil properties:	9,44E-02	[W/mK]
Duplex steel	20	[W/mK]
Concrete coating	1,5	[W/mK]
Sea water properties:	0,65	[W/mK]
Thermal conductivity of mud	0,6	[W/mK]
Oil properties:		
Density	609,8	[kg/m ³]
Volume Flowrate, q	0,15	[m ³ /s]
Mass flowrate	89	[kg/s]
Heat capacity	2416	[J/kgK]
Viscosity	3E-04	[Pas]
Temperature	70	[°C]
Average speed	2	[m/s]
Sea water properties:		
Temperature	4	[°C]
Heat capacity	4200	[J/kgK]
Viscosity	1E-03	[Pas]
Density	1020	[kg/m ³]
Average velocity	0,1	[m/s]
Wax:		
Heterogeneity coefficient	3	
Mud:		
Thickness	0,0150	[m]
Burial depth	0,4898	[m]

Table 2: Temperature profile cases.

Temperature profile							
	Case 1	Case 2	Case 3	Case 4	Case 5	Case 6	Case 7
Deposit Thickness [m]	0	0	0,005	0,005	0,01	0,01	0,01
Volume of oil in deposit	0	0	0,3	0,9	0,3	0,6	0,9
Buried	NO	YES	NO	NO	NO	NO	NO

Table 3: Typical Compositions of Petroleum Reservoir Fluids. (Gudmundsson, Produced and Processed Naturgass, 2011)

Component	Gas	Gas Condensate	Volatile Oil	Black Oil
N ₂	0.3	0.71	1.67	0.67
CO ₂	1.1	8.65	2.18	2.11
C ₁	90.0	70.86	60.51	34.93
C ₂	4.9	8.53	7.52	7.00
C ₃	1.9	4.95	4.74	7.82
C ₄ (i + n)	1.1	2.00	4.12	5.48
C ₅ (i + n)	0.4	0.81	2.97	3.80
C ₆ (i + n)	6 + : 0.3	0.46	1.99	3.04
C ₇		0.61	2.45	4.39
C ₈		0.71	2.41	4.71
C ₉		0.39	1.69	3.21
C ₁₀		0.28	1.42	1.79
C ₁₁		0.20	1.02	1.72
C ₁₂		0.15	12 + : 5.31	1.74
C ₁₃		0.11		1.74
C ₁₄		0.10		1.35
C ₁₅		0.07		1.34
C ₁₆		0.05		1.06
C ₁₇		17 + : 0.37		1.02
C ₁₈				1.00
C ₁₉				0.90
C ₂₀				20 + : 9.18

12. Figures

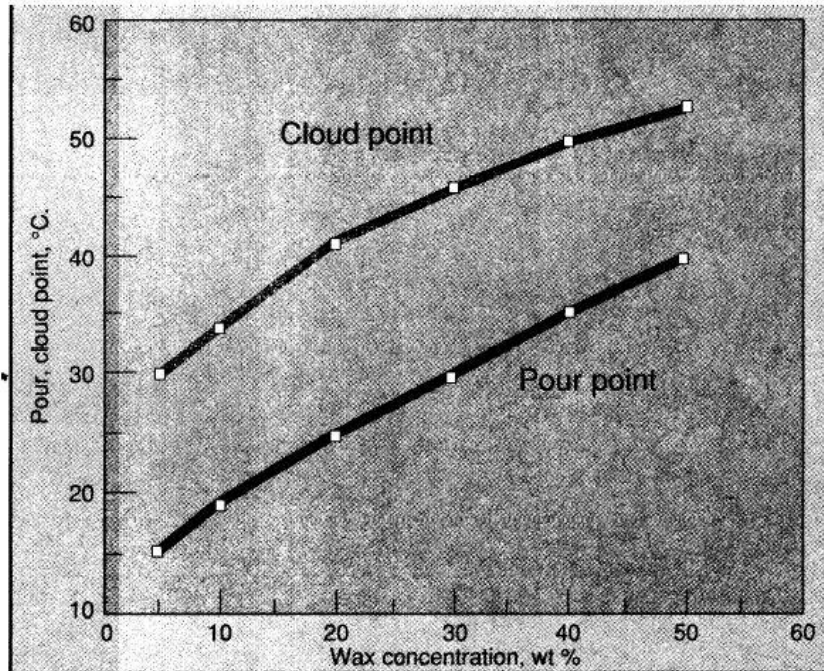


Figure 1: The cloud point and pour point of refined oil with different wax concentrations. (Gudmundsson, Pipeline Flow Assurance, 2010)

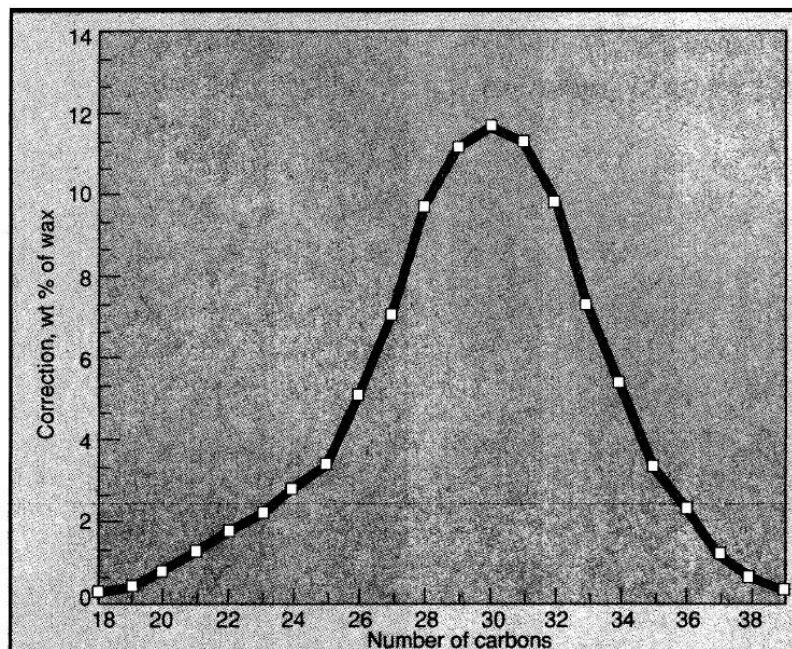


Figure 2: Shows the distribution and the range of hydrocarbons found in paraffin wax (Gudmundsson, Pipeline Flow Assurance, 2010)

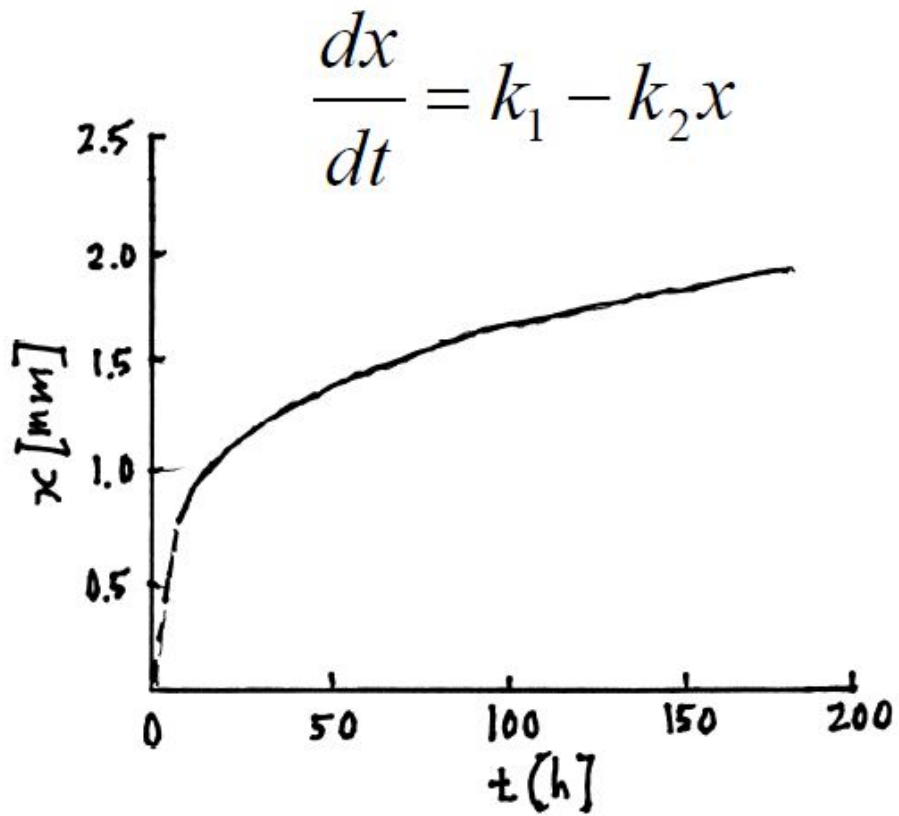


Figure 3: Wax deposit building up with time until there is no active temperature driving force (Gudmundsson, Pipeline Flow Assurance, 2010).

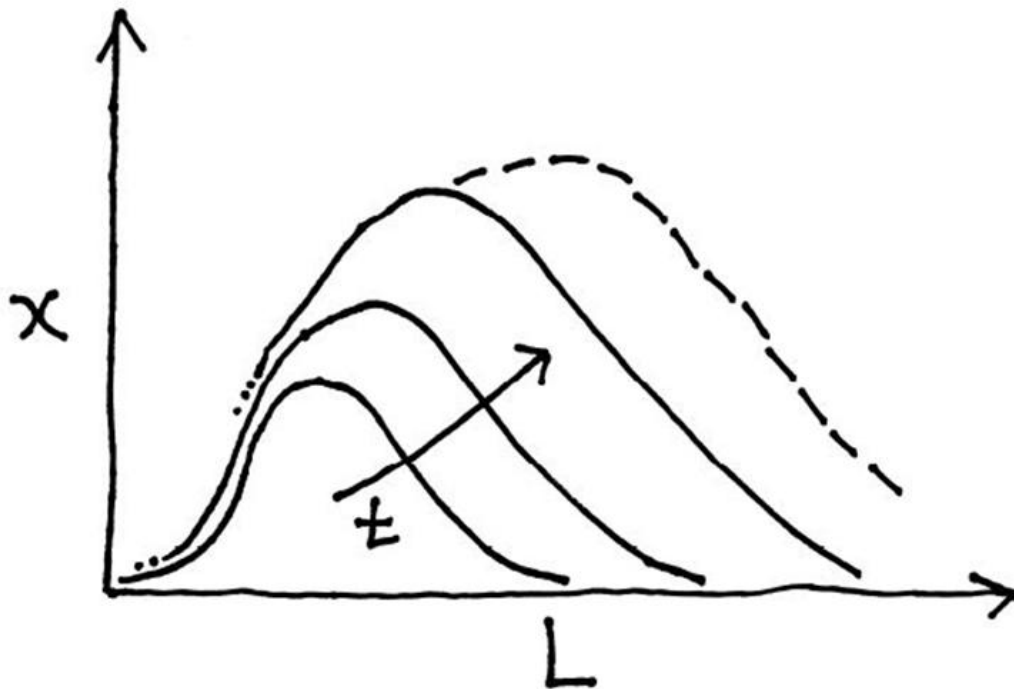


Figure 4: Wax deposits building up and moving down the pipeline with time (Gudmundsson, Pipeline Flow Assurance, 2010).

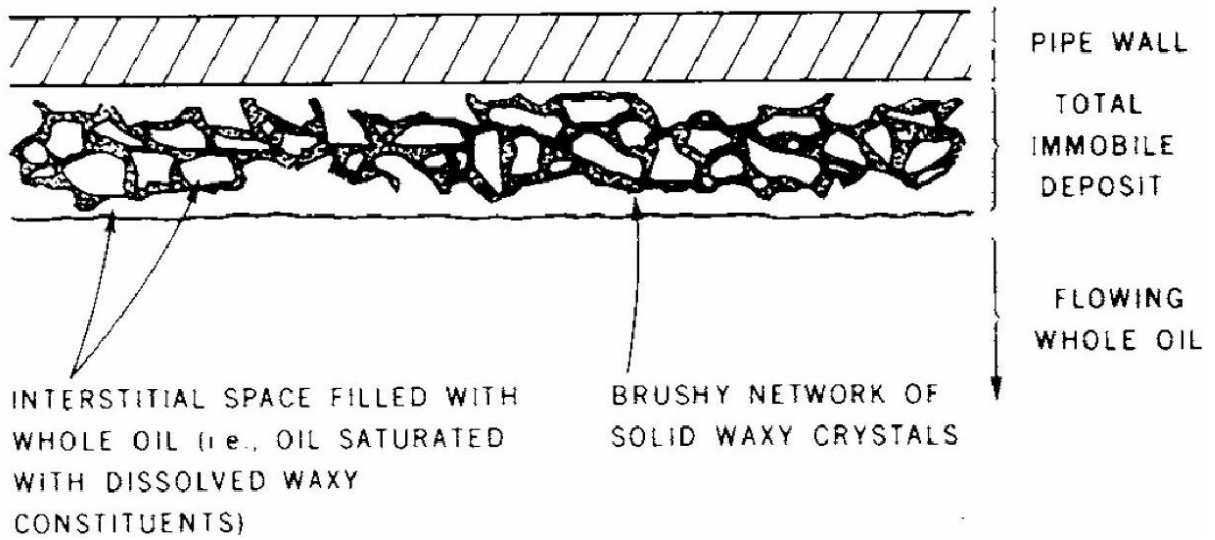


Figure 5: 3D-network of wax containing pores with oil (Burger, et al., 1981)

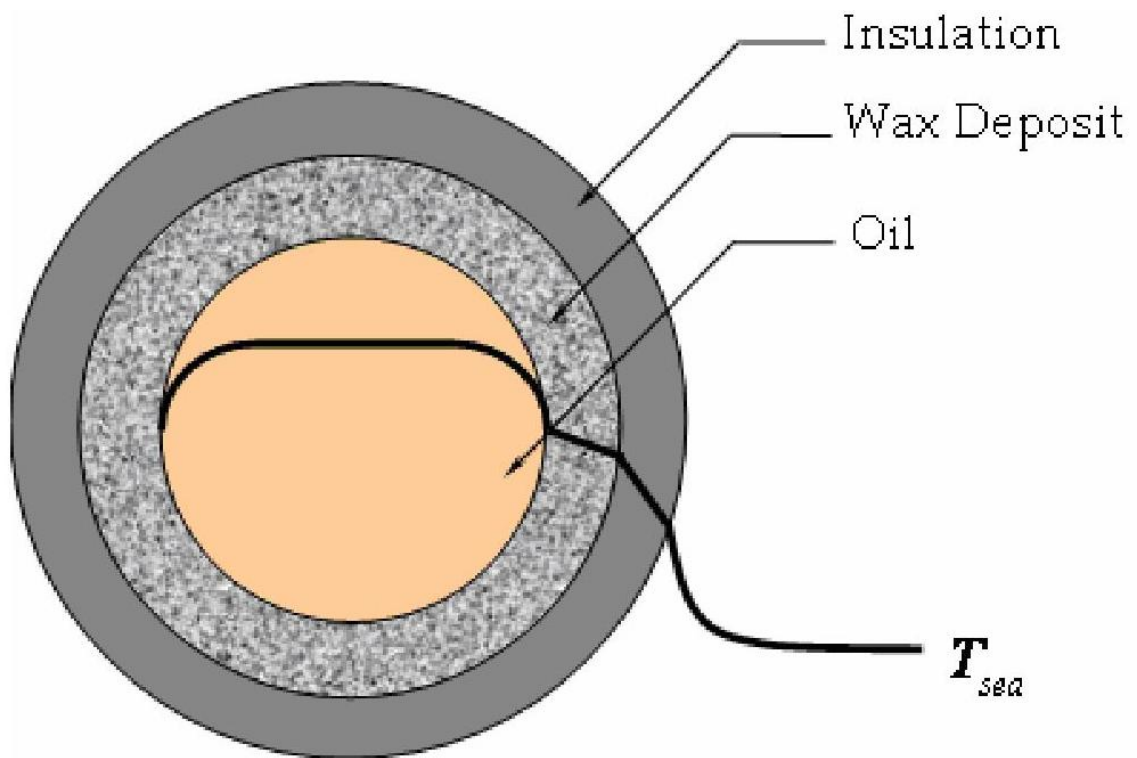


Figure 6: Cross-sectional temperature profile in a subsea pipeline (Rosvold, 2008).

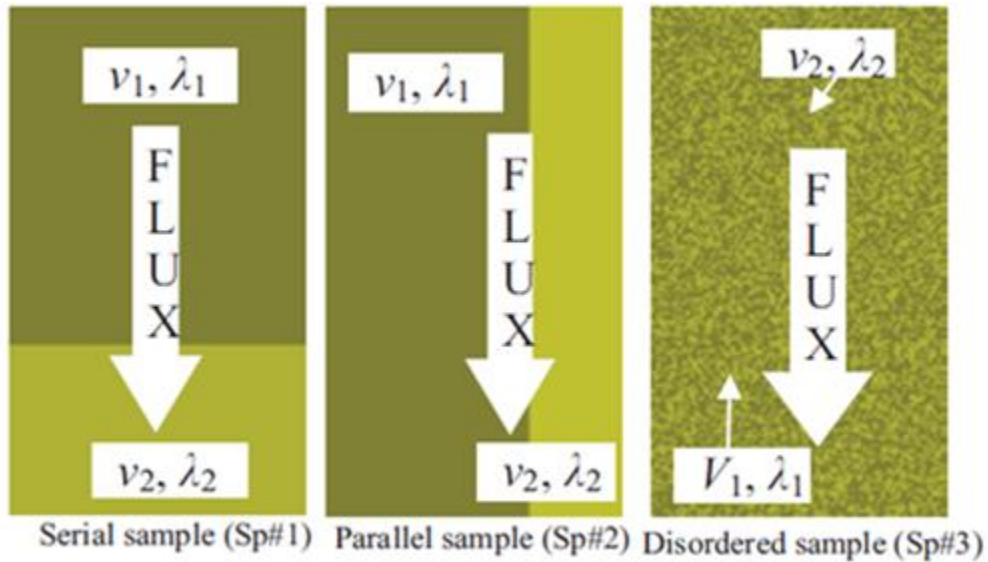


Figure 7: Two phase thermal conduct model. Three samples of different distribution of one medium in another medium (Tang, et al., 2009).

Woodside-Messmer Model: $\lambda_{eff} = \lambda_1^{v_1} \cdot \lambda_2^{v_2}$

Maxwell-Hamilton Model:

$$\lambda_{eff} = \lambda_1 \frac{(n-1)\lambda_1 + \lambda_2 - (n-1)(\lambda_1 - \lambda_2)v_2}{(n-1)\lambda_1 + \lambda_2 + (\lambda_1 - \lambda_2)v_2}$$

Figure 8: Theoretical thermal conductivity models for discontinuous two phase distribution (Tang, et al., 2009).

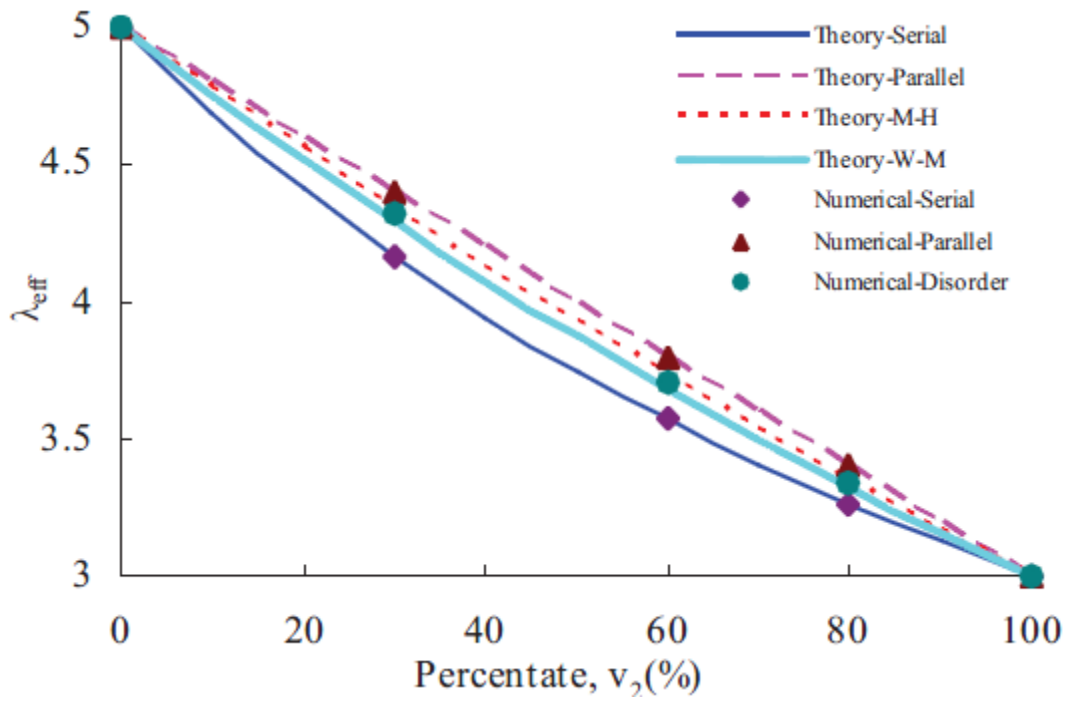


Figure 9: Theoretical and numerical obtained effective thermal conductivities over a range of V_2 for two phase mixtures.

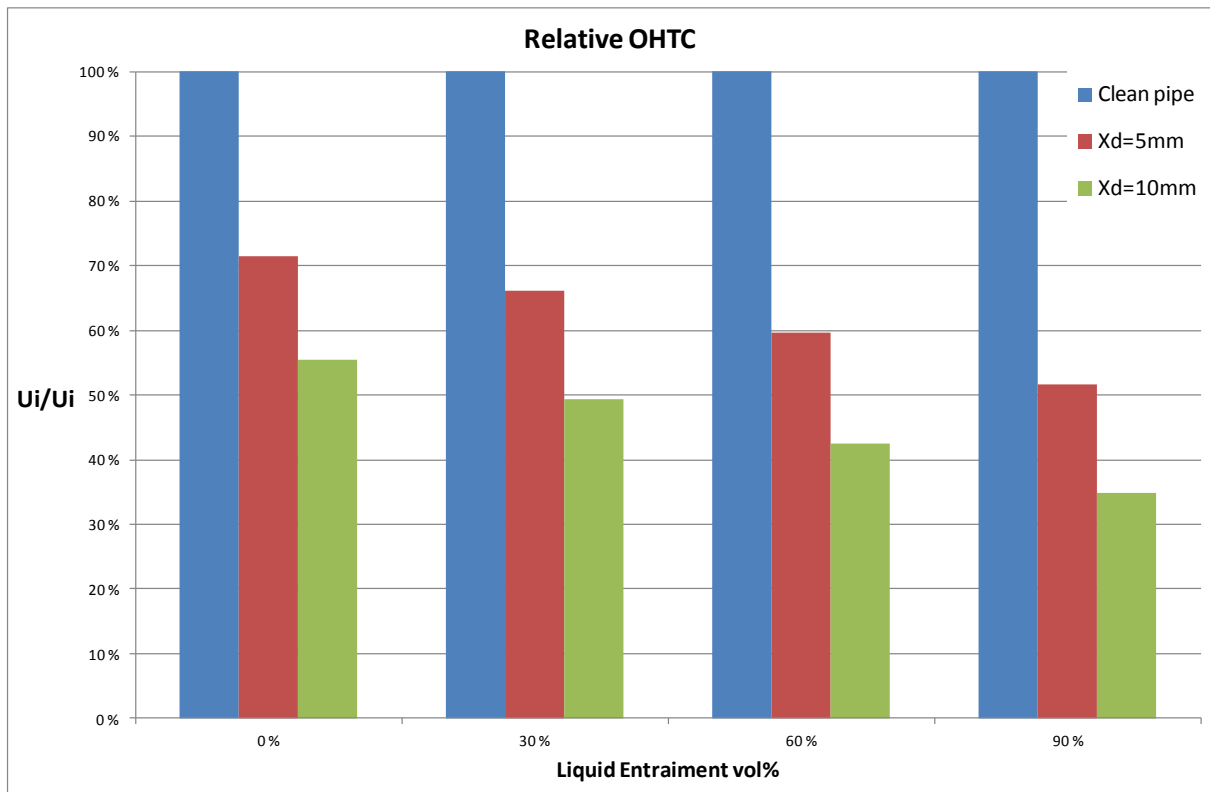


Figure 10: OHTC for selected wax thicknesses divided by OHTC for a clean pipe, with different of liquid volume %.

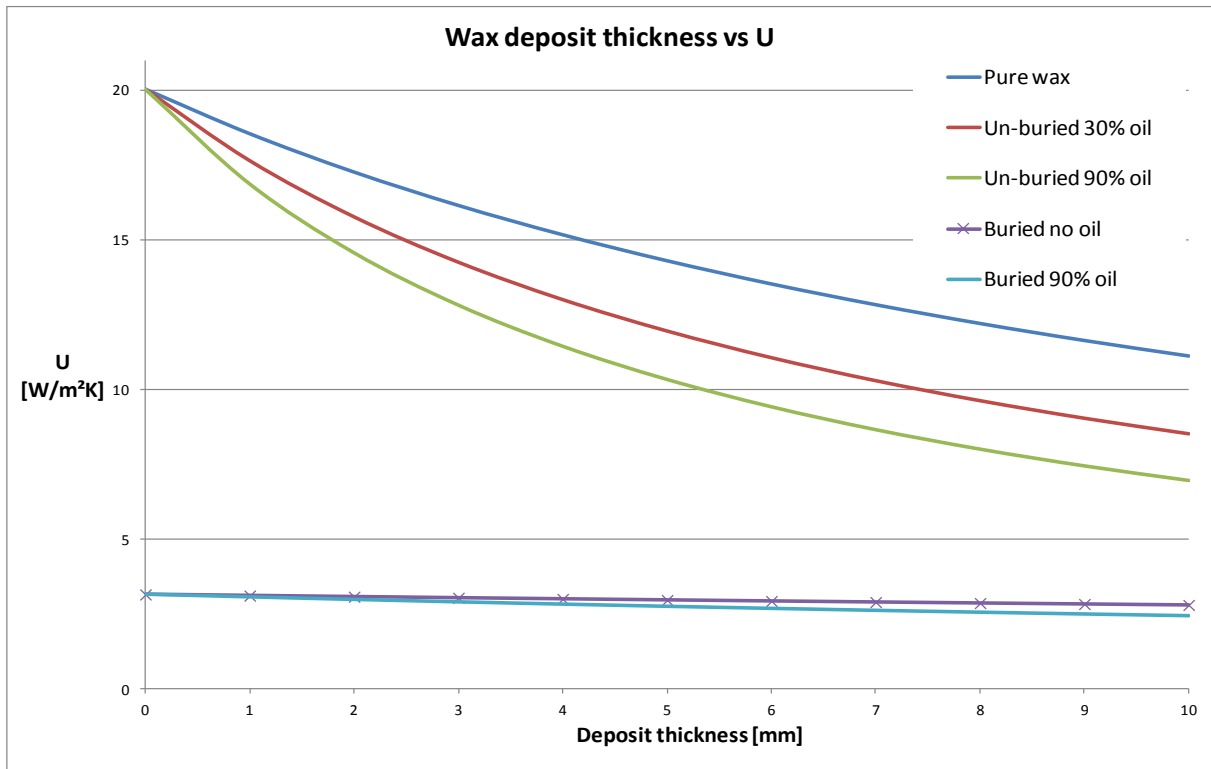


Figure 11: Wax deposit thickness vs. U

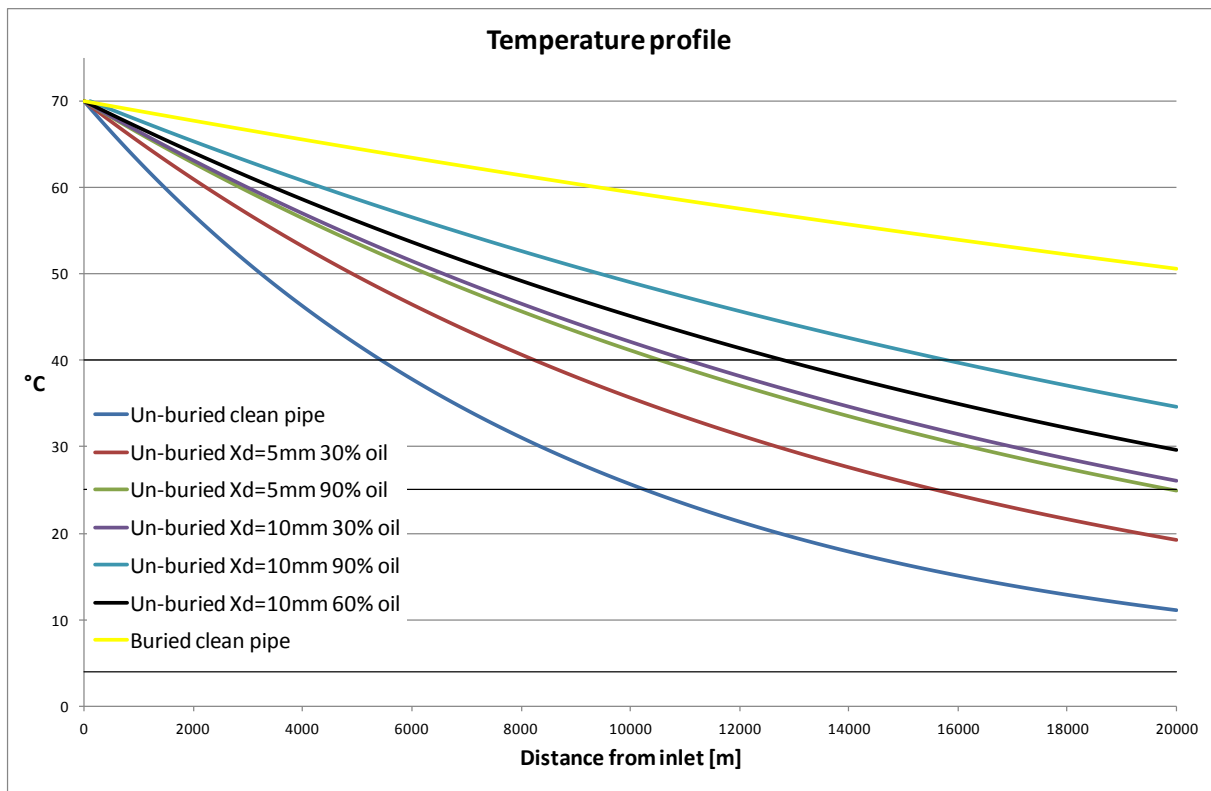


Figure 12: Subsea pipeline temperature profile. Horizontal lines are cloud point, pour point and ambient temperature from top to bottom.

13. Formulas

$$k_{avg} = k_{wax} \left[\frac{2k_{wax} + k_{oil} - 2(k_{wax} - k_{oil})V_{oil}}{2k_{wax} + k_{oil} + (k_{wax} - k_{oil})V_{oil}} \right]$$

Formula 1: Maxwell-Eucken model for effective thermal conductivity in wax deposits.

$$Nu = \frac{hd}{k}$$

Formula 2: Nusselt number.

$$Re = \frac{\rho ud}{\mu}$$

Formula 3: Reynolds number.

$$Pr = \frac{C_p \mu}{k}$$

Formula 4: Prandtl number.

$$Nu = 0,023 Re^{0,8} Pr^{0,33}$$

Formula 5: Dimensionless relationship for pipe flow (Gudmundsson, 2010).

$$Nu = 0,3 + \frac{0,62 Re^{1/2} Pr^{1/3}}{[1 + (0,4 / Pr)^{2/3}]^{1/4}} \left[1 + \left(\frac{Re}{282000} \right)^{5/8} \right]^{4/5}$$

Formula 6: The Churchill-Berstein equation (Mehrotra, et al., 2004)

$$U_i = \left\{ ID \cdot \sum \left(\frac{\ln \left(\frac{ID_{n+1}}{ID_n} \right)}{2 \cdot k_n} \right) + \frac{1}{h_i} + R_{fi} + \left(R_{fu} + \frac{1}{h_o} \right) \frac{ID}{OD} \right\}^{-1}$$

Formula 7: Overall heat transfer coefficient for a subsea pipeline.

$$U_i = \left\{ ID \cdot \sum \left(\frac{\ln \left(\frac{ID_{n+1}}{ID_n} \right)}{2 \cdot k_n} \right) + \frac{1}{h_i} + R_{fi} + \frac{ID}{OD} \cdot \frac{OD \cdot ACOSH \left(\frac{2 \cdot H}{OD} \right)}{k_{soil}} \right\}^{-1}$$

Formula 8: Overall heat transfer coefficient for a completely buried subsea pipeline (Loch, 2000).

$$h_{o,partly} = (1-f)h_{o,buried} + fh_{o,exposed}$$

Formula 9: Heat transfer coefficient for partly buried pipe (Bai & Bai, 2010).

$$T_2 = T_a + (T_{inlet} - T_a) \exp \left[\frac{-U \pi d}{m C_p} L \right]$$

Formula 10: The bulk temperature in steady-state pipeline flow with constant ambient temperature (Gudmundsson, 2010).

$$R_n = ID \left(\frac{\ln \left(\frac{ID_{n+1}}{ID_n} \right)}{2 \cdot k_n} \right)$$

Formula 11: Heat transfer resistance for pipe layer n.

$$R_{soil} = ID \left(\frac{ACOSH \left(\frac{2H}{OD} \right)}{2 \cdot k_n} \right)$$

Formula 12: Heat transfer resistance in soil.

14. Appendices

14.1 Re-writing to Maxwell-Eucken

The equation for induced magnetization found in Conduction of Heat in Solids is the same equation as the Maxwell-Hamilton equation with a heterogeneity coefficient of 3, also known as the Maxwell-Eucken model. To show this some algebra is applied to the equation found in (Carslaw, et al., 1959). The equation (Formula 13) is now exactly the same as Formula 1; Maxwell-Eucken model for effective thermal conductivity for any system consisting of continuous and discontinuous phase (spherical).

$$K_{eff} = \frac{3K_2K\alpha + (2K_1 + K_2)(K)(1-\alpha)}{3K_1\alpha + (2K_1 + K_2)(1-\alpha)}$$
$$K_{eff} = K_1 \frac{3K_2V_2 + 2K_1 - 2K_1V_2 + K_2 - K_2V_2}{3K_1V_2 + 2K_1 - 2K_1V_2 + K_2 - K_2V_2}$$
$$K_{eff} = K_1 \frac{V_2(2K_2 - 2K_1) + 2K_1 + K_2}{V_2(K_1 - K_2) + 2K_1 + K_2}$$
$$K_{eff} = K_1 \frac{2K_1 + K_2 - 2(K_1 - K_2)V_2}{2K_1 + K_2 + (K_1 - K_2)V_2}$$

Formula 13: Re-writing to the form of Maxwell-Eucken model. $\alpha = V_2$.

14.2 Calculation data references

The data in Table 1 is either from literature, HYSYS or assumed. Here is an explanation of where the different values come from: All the information about sea water is taken from (Mehrotra, et al., 2004). By entering the flow rate, pressure, oil composition and temperature into HYSYS information about the density, heat capacity, thermal conductivity and viscosity of the volatile oil flow were found. The conductivity of duplex steel and concrete are taken from (Gudmundsson, 2009). I found information about average speed and water-saturated mud in the appendix to Solids in Oil and Gas Production (Gudmundsson, 2010). The heterogeneity coefficient was found in the paper of (Tang, et al., 2009). And I assumed the values for burial depth, concrete thickness, inner diameter, length of the pipeline, mud thickness and inlet temperature. I used the thermal conductivity of paraffin wax from (Toolbox).

14.3 Calculation procedure

Procedure: After finding credible data and gathering them in Table 1 and deciding on which formulas to use I could calculate the values I needed. First I used the volume% from table 4 and the wax and oil thermal conductivity from Table 1 in Formula 1 to calculate the thermal conductivity of the wax deposit. Then I subtracted the deposition thickness from the clean pipe inner diameter to find the new flow diameter for all thicknesses. I used the diameter to calculate flow average speed, and used the speed to calculate the Reynolds numbers (Re).

I continued by calculating the other dimensionless numbers for the pipeline's inside and outside by the use of data from Table 1. The paraffin wax's fouling resistance was then calculated by dividing the wax layer's thickness by the corresponding thermal conductivity. R_v and R_c is the heat transfer resistance in steel pipe and the anti-floating concrete layer. It is calculated with Formula 12. h_v and h_c are the inverse of R_v and R_c . R_{fo} are calculated by dividing assumed water-saturated thickness with its thermal conductivity found in Table 1. R_{soil} is calculated by formula 13. Finally I could calculate OHTC for buried and un-buried pipeline with Formula 7 and Formula 8. The temperature profile was made by the use of Formula 10.

Table 4: Calculated values for deposit conductivity, flow parameters and dimensionless parameters for conduction and heat resistance/heat transfer coefficient in the laminar sub-layer and on the pipeline's outside.

Deposit Thickness	0,00E+00	1,00E-03	2,00E-03	3,00E-03	4,00E-03	5,00E-03	6,00E-03	7,00E-03	8,00E-03	9,00E-03	1,00E-02
Volume% of oil in deposit	Volume% of oil in deposit	Volume% of oil in deposit	Volume% of oil in deposit	Volume% of oil in deposit	Volume% of oil in deposit	Volume% of oil in deposit	Volume% of oil in deposit	Volume% of oil in deposit	Volume% of oil in deposit	Volume% of oil in deposit	Volume% of oil in deposit
0	0	0	0	0	0	0	0	0	0	0	0
0,3	0,3	0,3	0,3	0,3	0,3	0,3	0,3	0,3	0,3	0,3	0,3
0,6	0,6	0,6	0,6	0,6	0,6	0,6	0,6	0,6	0,6	0,6	0,6
0,9	0,9	0,9	0,9	0,9	0,9	0,9	0,9	0,9	0,9	0,9	0,9

Thermal conductivity deposit [W/mK]	Thermal conductivity deposit [W/mK]	Thermal conductivity deposit [W/mK]	Thermal conductivity deposit [W/mK]	Thermal conductivity deposit [W/mK]	Thermal conductivity deposit [W/mK]	Thermal conductivity deposit [W/mK]	Thermal conductivity deposit [W/mK]	Thermal conductivity deposit [W/mK]	Thermal conductivity deposit [W/mK]	Thermal conductivity deposit [W/mK]	Thermal conductivity deposit [W/mK]
0,250	0,250	0,250	0,250	0,250	0,250	0,250	0,250	0,250	0,250	0,250	0,250
0,195	0,195	0,195	0,195	0,195	0,195	0,195	0,195	0,195	0,195	0,195	0,195
0,148	0,148	0,148	0,148	0,148	0,148	0,148	0,148	0,148	0,148	0,148	0,148
0,107	0,107	0,107	0,107	0,107	0,107	0,107	0,107	0,107	0,107	0,107	0,107

Flow diameter	0,305	0,304	0,303	0,302	0,301	0,300	0,299	0,298	0,297	0,296	0,295
Flow radius	0,152	0,152	0,151	0,151	0,150	0,150	0,149	0,149	0,148	0,148	0,147
Area	0,073	0,072	0,072	0,072	0,071	0,071	0,070	0,070	0,069	0,069	0,068
Average speed	2,000	2,013	2,027	2,040	2,054	2,067	2,081	2,095	2,109	2,124	2,138

BULK FLOW

Pr	6,4	6,4	6,4	6,4	6,4	6,4	6,4	6,4	6,4	6,4	6,4
Re	1,48E+06	1,48E+06	1,49E+06	1,49E+06	1,50E+06	1,50E+06	1,51E+06	1,51E+06	1,52E+06	1,52E+06	1,53E+06
Nu	3,67E+03	3,68E+03	3,69E+03	3,70E+03	3,71E+03	3,72E+03	3,73E+03	3,74E+03	3,75E+03	3,76E+03	3,77E+03
hi	1136	1143	1149	1156	1163	1170	1177	1184	1191	1199	1206
Ri	8,80E-04	8,75E-04	8,70E-04	8,65E-04	8,60E-04	8,55E-04	8,49E-04	8,44E-04	8,39E-04	8,34E-04	8,29E-04

SEA WATER

Pr	6,5	6,5	6,5	6,5	6,5	6,5	6,5	6,5	6,5	6,5	6,5
Re	3,87E+04	3,87E+04	3,87E+04	3,87E+04	3,87E+04	3,87E+04	3,87E+04	3,87E+04	3,87E+04	3,87E+04	3,87E+04
Nu	2,69E+02	2,69E+02	2,69E+02	2,69E+02	2,69E+02	2,69E+02	2,69E+02	2,69E+02	2,69E+02	2,69E+02	2,69E+02
Un-buried hu	460	460	460	460	460	460	460	460	460	460	460
Ru	2,17E-03	2,17E-03	2,17E-03	2,17E-03	2,17E-03	2,17E-03	2,17E-03	2,17E-03	2,17E-03	2,17E-03	2,17E-03

Fouling resistance, R	0	4,00E-03	8,00E-03	1,20E-02	1,60E-02	2,00E-02	2,40E-02	2,80E-02	3,20E-02	3,60E-02	4,00E-02
Fouling resistance, R	0	5,12E-03	1,02E-02	1,54E-02	2,05E-02	2,56E-02	3,07E-02	3,58E-02	4,09E-02	4,61E-02	5,12E-02
Fouling resistance, R	0	6,75E-03	1,35E-02	2,02E-02	2,70E-02	3,37E-02	4,05E-02	4,72E-02	5,40E-02	6,07E-02	6,75E-02
Fouling resistance, R	0	9,35E-03	1,87E-02	2,80E-02	3,74E-02	4,67E-02	5,61E-02	6,54E-02	7,48E-02	8,41E-02	9,35E-02

Rv	5,78E-04	[m ² K/W]
hv	1731	[W/m ² K]
Rc	1,46E-02	[m ² K/W]
hc	68,51	[W/m ² K]
Rsoil	0,38	[m ² K/W]
Hsoil	2,66	[W/m ² K]
Rfo	0,03	[m ² K/W]

Un-Buried

Overall heat transfer coefficient											
U	20,04	18,55	17,27	16,16	15,18	14,31	13,53	12,84	12,21	11,64	11,12
	20,04	18,18	16,63	15,33	14,21	13,25	12,41	11,67	11,01	10,42	9,89
	20,04	17,65	15,77	14,26	13,01	11,96	11,06	10,30	9,63	9,04	8,52
	20,04	16,88	14,58	12,83	11,46	10,35	9,44	8,67	8,02	7,46	6,98

Buried

Overall heat transfer coefficient											
U	3,15	3,11	3,07	3,04	3,00	2,96	2,93	2,90	2,86	2,83	2,80
	3,15	3,10	3,05	3,01	2,96	2,92	2,87	2,83	2,79	2,75	2,71
	3,15	3,08	3,02	2,96	2,90	2,85	2,79	2,74	2,69	2,64	2,60
	3,15	3,06	2,98	2,89	2,82	2,75	2,68	2,61	2,55	2,49	2,43

Table 5: Temperature profile table

Temperatur profile									
	0 mm	5 mm		10 mm		0 mm	5 mm	10 mm	10 mm
	0	30 %	90 %	30 %	90 %	Buried	60 %	60 %	Buried and 90%
L	T2	T2	T2	T2	T2	T2	T2	T2	T2
0	70	70	70	70	70	70	70,00	70,00	70
100	69,27	69,52	69,62	69,64	69,75	69,88	69,56	69,69	69,91
200	68,55	69,04	69,25	69,28	69,49	69,77	69,13	69,38	69,82
300	67,84	68,56	68,87	68,92	69,24	69,65	68,70	69,07	69,73
400	67,13	68,09	68,50	68,57	68,99	69,54	68,27	68,76	69,64
500	66,43	67,62	68,13	68,21	68,74	69,43	67,85	68,46	69,56
600	65,74	67,15	67,77	67,86	68,49	69,31	67,43	68,15	69,47
700	65,06	66,69	67,40	67,51	68,24	69,20	67,01	67,85	69,38
800	64,38	66,23	67,04	67,17	67,99	69,08	66,59	67,55	69,29
900	63,72	65,78	66,68	66,82	67,74	68,97	66,18	67,25	69,20
1000	63,06	65,32	66,32	66,48	67,50	68,86	65,76	66,95	69,11
1100	62,40	64,88	65,96	66,13	67,25	68,74	65,36	66,66	69,03
1200	61,76	64,43	65,61	65,79	67,01	68,63	64,95	66,36	68,94
1300	61,12	63,99	65,25	65,46	66,76	68,52	64,55	66,07	68,85
1400	60,49	63,55	64,90	65,12	66,52	68,40	64,15	65,77	68,76
1500	59,86	63,11	64,55	64,78	66,28	68,29	63,75	65,48	68,68
1600	59,25	62,68	64,21	64,45	66,04	68,18	63,36	65,19	68,59
1700	58,63	62,25	63,86	64,12	65,80	68,07	62,96	64,91	68,50
1800	58,03	61,82	63,52	63,79	65,56	67,96	62,57	64,62	68,42
1900	57,43	61,40	63,18	63,46	65,32	67,84	62,19	64,33	68,33
2000	56,84	60,98	62,84	63,14	65,09	67,73	61,80	64,05	68,24
2100	56,26	60,56	62,50	62,82	64,85	67,62	61,42	63,76	68,16
2200	55,68	60,15	62,17	62,49	64,61	67,51	61,04	63,48	68,07
2300	55,11	59,74	61,84	62,17	64,38	67,40	60,66	63,20	67,98
2400	54,54	59,33	61,51	61,86	64,15	67,29	60,29	62,92	67,90
2500	53,99	58,92	61,18	61,54	63,91	67,18	59,92	62,65	67,81
2600	53,43	58,52	60,85	61,22	63,68	67,07	59,55	62,37	67,72
2700	52,89	58,12	60,52	60,91	63,45	66,96	59,18	62,09	67,64
2800	52,35	57,73	60,20	60,60	63,22	66,85	58,81	61,82	67,55
2900	51,81	57,33	59,88	60,29	62,99	66,74	58,45	61,55	67,47
3000	51,28	56,94	59,56	59,98	62,77	66,63	58,09	61,28	67,38
3100	50,76	56,56	59,24	59,68	62,54	66,52	57,73	61,01	67,29
3200	50,24	56,17	58,92	59,37	62,31	66,41	57,38	60,74	67,21
3300	49,73	55,79	58,61	59,07	62,09	66,30	57,03	60,47	67,12
3400	49,23	55,41	58,30	58,77	61,86	66,19	56,68	60,20	67,04
3500	48,73	55,03	57,99	58,47	61,64	66,08	56,33	59,94	66,95
3600	48,23	54,66	57,68	58,17	61,42	65,98	55,98	59,68	66,87
3700	47,74	54,29	57,37	57,87	61,20	65,87	55,64	59,41	66,78
3800	47,26	53,92	57,07	57,58	60,98	65,76	55,30	59,15	66,70
3900	46,78	53,55	56,76	57,28	60,76	65,65	54,96	58,89	66,61
4000	46,31	53,19	56,46	56,99	60,54	65,54	54,62	58,63	66,53
4100	45,84	52,83	56,16	56,70	60,32	65,44	54,29	58,37	66,45
4200	45,38	52,47	55,86	56,41	60,10	65,33	53,95	58,12	66,36
4300	44,92	52,12	55,56	56,13	59,88	65,22	53,62	57,86	66,28
4400	44,47	51,77	55,27	55,84	59,67	65,12	53,30	57,61	66,19
4500	44,02	51,42	54,98	55,56	59,45	65,01	52,97	57,36	66,11
4600	43,58	51,07	54,68	55,28	59,24	64,90	52,65	57,11	66,03
4700	43,14	50,73	54,39	55,00	59,03	64,80	52,32	56,85	65,94
4800	42,71	50,38	54,10	54,72	58,81	64,69	52,01	56,61	65,86
4900	42,28	50,04	53,82	54,44	58,60	64,58	51,69	56,36	65,78
5000	41,86	49,71	53,53	54,16	58,39	64,48	51,37	56,11	65,69

5000	41,86	49,71	53,53	54,16	58,39	64,48	51,37	56,11	65,69
5100	41,44	49,37	53,25	53,89	58,18	64,37	51,06	55,87	65,61
5200	41,02	49,04	52,97	53,61	57,97	64,27	50,75	55,62	65,53
5300	40,62	48,71	52,69	53,34	57,76	64,16	50,44	55,38	65,44
5400	40,21	48,38	52,41	53,07	57,56	64,06	50,13	55,14	65,36
5500	39,81	48,06	52,13	52,80	57,35	63,95	49,83	54,89	65,28
5600	39,41	47,74	51,86	52,54	57,14	63,85	49,52	54,65	65,19
5700	39,02	47,42	51,58	52,27	56,94	63,74	49,22	54,42	65,11
5800	38,64	47,10	51,31	52,01	56,73	63,64	48,93	54,18	65,03
5900	38,25	46,78	51,04	51,75	56,53	63,53	48,63	53,94	64,95
6000	37,87	46,47	50,77	51,48	56,33	63,43	48,33	53,71	64,86
6100	37,50	46,16	50,50	51,22	56,12	63,33	48,04	53,47	64,78
6200	37,13	45,85	50,24	50,97	55,92	63,22	47,75	53,24	64,70
6300	36,76	45,54	49,97	50,71	55,72	63,12	47,46	53,01	64,62
6400	36,40	45,24	49,71	50,45	55,52	63,02	47,17	52,77	64,54
6500	36,04	44,94	49,45	50,20	55,32	62,91	46,89	52,54	64,46
6600	35,69	44,64	49,19	49,95	55,13	62,81	46,60	52,32	64,37
6700	35,34	44,34	48,93	49,69	54,93	62,71	46,32	52,09	64,29
6800	34,99	44,04	48,67	49,44	54,73	62,61	46,04	51,86	64,21
6900	34,65	43,75	48,41	49,20	54,54	62,50	45,76	51,64	64,13
7000	34,31	43,46	48,16	48,95	54,34	62,40	45,49	51,41	64,05
7100	33,98	43,17	47,91	48,70	54,15	62,30	45,21	51,19	63,97
7200	33,64	42,88	47,66	48,46	53,95	62,20	44,94	50,97	63,89
7300	33,32	42,60	47,41	48,21	53,76	62,10	44,67	50,74	63,81
7400	32,99	42,32	47,16	47,97	53,57	61,99	44,40	50,52	63,73
7500	32,67	42,04	46,91	47,73	53,38	61,89	44,14	50,30	63,64
7600	32,35	41,76	46,67	47,49	53,19	61,79	43,87	50,09	63,56
7700	32,04	41,48	46,42	47,25	53,00	61,69	43,61	49,87	63,48
7800	31,73	41,21	46,18	47,02	52,81	61,59	43,34	49,65	63,40
7900	31,42	40,93	45,94	46,78	52,62	61,49	43,08	49,44	63,32
8000	31,12	40,66	45,70	46,55	52,43	61,39	42,83	49,22	63,24
8100	30,82	40,40	45,46	46,32	52,24	61,29	42,57	49,01	63,16
8200	30,52	40,13	45,22	46,08	52,06	61,19	42,31	48,80	63,08
8300	30,23	39,86	44,98	45,85	51,87	61,09	42,06	48,59	63,00
8400	29,94	39,60	44,75	45,62	51,69	60,99	41,81	48,38	62,92
8500	29,65	39,34	44,52	45,40	51,50	60,89	41,56	48,17	62,84
8600	29,37	39,08	44,29	45,17	51,32	60,79	41,31	47,96	62,77
8700	29,09	38,83	44,05	44,94	51,14	60,69	41,06	47,75	62,69
8800	28,81	38,57	43,83	44,72	50,95	60,59	40,82	47,55	62,61
8900	28,54	38,32	43,60	44,50	50,77	60,49	40,58	47,34	62,53
9000	28,27	38,07	43,37	44,28	50,59	60,39	40,33	47,14	62,45
9100	28,00	37,82	43,15	44,06	50,41	60,30	40,09	46,93	62,37
9200	27,73	37,57	42,92	43,84	50,23	60,20	39,86	46,73	62,29
9300	27,47	37,32	42,70	43,62	50,05	60,10	39,62	46,53	62,21
9400	27,21	37,08	42,48	43,40	49,88	60,00	39,38	46,33	62,13
9500	26,96	36,84	42,26	43,19	49,70	59,90	39,15	46,13	62,06
9600	26,70	36,60	42,04	42,97	49,52	59,81	38,92	45,93	61,98
9700	26,45	36,36	41,82	42,76	49,35	59,71	38,69	45,73	61,90
9800	26,20	36,12	41,60	42,55	49,17	59,61	38,46	45,54	61,82
9900	25,96	35,89	41,39	42,34	49,00	59,51	38,23	45,34	61,74
10000	25,71	35,65	41,17	42,13	48,82	59,42	38,00	45,14	61,67

10100	25,47	35,42	40,96	41,92	48,65	59,32	37,78	44,95	61,59
10200	25,24	35,19	40,75	41,71	48,48	59,22	37,55	44,76	61,51
10300	25,00	34,96	40,54	41,50	48,31	59,13	37,33	44,57	61,43
10400	24,77	34,74	40,33	41,30	48,14	59,03	37,11	44,37	61,35
10500	24,54	34,51	40,12	41,09	47,97	58,94	36,89	44,18	61,28
10600	24,31	34,29	39,92	40,89	47,80	58,84	36,68	43,99	61,20
10700	24,09	34,07	39,71	40,69	47,63	58,74	36,46	43,81	61,12
10800	23,87	33,85	39,51	40,49	47,46	58,65	36,25	43,62	61,05
10900	23,65	33,63	39,30	40,29	47,29	58,55	36,03	43,43	60,97
11000	23,43	33,41	39,10	40,09	47,12	58,46	35,82	43,25	60,89
11100	23,22	33,20	38,90	39,89	46,96	58,36	35,61	43,06	60,82
11200	23,00	32,98	38,70	39,70	46,79	58,27	35,40	42,88	60,74
11300	22,79	32,77	38,50	39,50	46,63	58,17	35,19	42,69	60,66
11400	22,58	32,56	38,30	39,31	46,46	58,08	34,99	42,51	60,59
11500	22,38	32,35	38,11	39,11	46,30	57,98	34,78	42,33	60,51
11600	22,18	32,14	37,91	38,92	46,13	57,89	34,58	42,15	60,43
11700	21,98	31,94	37,72	38,73	45,97	57,80	34,38	41,97	60,36
11800	21,78	31,73	37,53	38,54	45,81	57,70	34,18	41,79	60,28
11900	21,58	31,53	37,33	38,35	45,65	57,61	33,98	41,61	60,20
12000	21,39	31,33	37,14	38,16	45,49	57,51	33,78	41,43	60,13
12100	21,19	31,13	36,95	37,98	45,33	57,42	33,58	41,26	60,05
12200	21,00	30,93	36,76	37,79	45,17	57,33	33,39	41,08	59,98
12300	20,82	30,73	36,58	37,60	45,01	57,23	33,19	40,91	59,90
12400	20,63	30,54	36,39	37,42	44,85	57,14	33,00	40,73	59,83
12500	20,45	30,34	36,20	37,24	44,69	57,05	32,81	40,56	59,75
12600	20,26	30,15	36,02	37,06	44,53	56,96	32,62	40,39	59,68
12700	20,08	29,96	35,84	36,87	44,38	56,86	32,43	40,22	59,60
12800	19,91	29,77	35,65	36,70	44,22	56,77	32,24	40,05	59,53
12900	19,73	29,58	35,47	36,52	44,07	56,68	32,05	39,88	59,45
13000	19,56	29,39	35,29	36,34	43,91	56,59	31,87	39,71	59,38
13100	19,38	29,21	35,11	36,16	43,76	56,50	31,68	39,54	59,30
13200	19,21	29,02	34,94	35,99	43,60	56,40	31,50	39,37	59,23
13300	19,05	28,84	34,76	35,81	43,45	56,31	31,32	39,20	59,15
13400	18,88	28,66	34,58	35,64	43,30	56,22	31,14	39,04	59,08
13500	18,72	28,48	34,41	35,46	43,15	56,13	30,96	38,87	59,00
13600	18,55	28,30	34,23	35,29	43,00	56,04	30,78	38,71	58,93
13700	18,39	28,12	34,06	35,12	42,85	55,95	30,60	38,54	58,86
13800	18,23	27,94	33,89	34,95	42,70	55,86	30,43	38,38	58,78
13900	18,08	27,77	33,72	34,78	42,55	55,77	30,25	38,22	58,71
14000	17,92	27,59	33,55	34,61	42,40	55,68	30,08	38,06	58,63
14100	17,77	27,42	33,38	34,44	42,25	55,59	29,91	37,90	58,56
14200	17,61	27,25	33,21	34,28	42,10	55,50	29,74	37,74	58,49
14300	17,46	27,08	33,04	34,11	41,95	55,41	29,57	37,58	58,41
14400	17,31	26,91	32,88	33,95	41,81	55,32	29,40	37,42	58,34
14500	17,17	26,74	32,71	33,78	41,66	55,23	29,23	37,26	58,27
14600	17,02	26,57	32,55	33,62	41,52	55,14	29,06	37,11	58,19
14700	16,88	26,41	32,38	33,46	41,37	55,05	28,90	36,95	58,12
14800	16,74	26,25	32,22	33,30	41,23	54,96	28,73	36,79	58,05
14900	16,59	26,08	32,06	33,14	41,08	54,87	28,57	36,64	57,97
15000	16,46	25,92	31,90	32,98	40,94	54,78	28,41	36,49	57,90

15100	16,32	25,76	31,74	32,82	40,80	54,69	28,25	36,33	57,83
15200	16,18	25,60	31,58	32,66	40,65	54,60	28,08	36,18	57,76
15300	16,05	25,44	31,42	32,50	40,51	54,52	27,93	36,03	57,68
15400	15,91	25,29	31,27	32,35	40,37	54,43	27,77	35,88	57,61
15500	15,78	25,13	31,11	32,19	40,23	54,34	27,61	35,73	57,54
15600	15,65	24,98	30,95	32,04	40,09	54,25	27,45	35,58	57,47
15700	15,52	24,82	30,80	31,88	39,95	54,16	27,30	35,43	57,39
15800	15,40	24,67	30,65	31,73	39,81	54,08	27,15	35,28	57,32
15900	15,27	24,52	30,49	31,58	39,68	53,99	26,99	35,13	57,25
16000	15,14	24,37	30,34	31,43	39,54	53,90	26,84	34,99	57,18
16100	15,02	24,22	30,19	31,28	39,40	53,81	26,69	34,84	57,11
16200	14,90	24,07	30,04	31,13	39,26	53,73	26,54	34,69	57,03
16300	14,78	23,92	29,89	30,98	39,13	53,64	26,39	34,55	56,96
16400	14,66	23,78	29,74	30,83	38,99	53,55	26,24	34,41	56,89
16500	14,54	23,63	29,60	30,69	38,86	53,47	26,10	34,26	56,82
16600	14,43	23,49	29,45	30,54	38,72	53,38	25,95	34,12	56,75
16700	14,31	23,35	29,31	30,40	38,59	53,29	25,80	33,98	56,68
16800	14,20	23,20	29,16	30,25	38,45	53,21	25,66	33,84	56,61
16900	14,08	23,06	29,02	30,11	38,32	53,12	25,52	33,70	56,54
17000	13,97	22,92	28,87	29,96	38,19	53,04	25,37	33,56	56,47
17100	13,86	22,79	28,73	29,82	38,06	52,95	25,23	33,42	56,39
17200	13,75	22,65	28,59	29,68	37,93	52,87	25,09	33,28	56,32
17300	13,65	22,51	28,45	29,54	37,79	52,78	24,95	33,14	56,25
17400	13,54	22,38	28,31	29,40	37,66	52,70	24,82	33,00	56,18
17500	13,43	22,24	28,17	29,26	37,53	52,61	24,68	32,87	56,11
17600	13,33	22,11	28,03	29,12	37,40	52,53	24,54	32,73	56,04
17700	13,23	21,98	27,89	28,99	37,28	52,44	24,41	32,59	55,97
17800	13,12	21,84	27,76	28,85	37,15	52,36	24,27	32,46	55,90
17900	13,02	21,71	27,62	28,71	37,02	52,27	24,14	32,33	55,83
18000	12,92	21,58	27,49	28,58	36,89	52,19	24,00	32,19	55,76
18100	12,82	21,46	27,35	28,44	36,76	52,10	23,87	32,06	55,69
18200	12,73	21,33	27,22	28,31	36,64	52,02	23,74	31,93	55,62
18300	12,63	21,20	27,08	28,18	36,51	51,94	23,61	31,80	55,55
18400	12,53	21,07	26,95	28,04	36,39	51,85	23,48	31,66	55,48
18500	12,44	20,95	26,82	27,91	36,26	51,77	23,35	31,53	55,41
18600	12,35	20,83	26,69	27,78	36,14	51,68	23,22	31,40	55,34
18700	12,26	20,70	26,56	27,65	36,01	51,60	23,10	31,27	55,27
18800	12,16	20,58	26,43	27,52	35,89	51,52	22,97	31,15	55,21
18900	12,07	20,46	26,30	27,39	35,77	51,44	22,84	31,02	55,14
19000	11,98	20,34	26,18	27,27	35,64	51,35	22,72	30,89	55,07
19100	11,90	20,22	26,05	27,14	35,52	51,27	22,60	30,76	55,00
19200	11,81	20,10	25,92	27,01	35,40	51,19	22,47	30,64	54,93
19300	11,72	19,98	25,80	26,89	35,28	51,10	22,35	30,51	54,86
19400	11,64	19,87	25,67	26,76	35,16	51,02	22,23	30,39	54,79
19500	11,55	19,75	25,55	26,64	35,04	50,94	22,11	30,26	54,72
19600	11,47	19,63	25,42	26,51	34,92	50,86	21,99	30,14	54,66
19700	11,39	19,52	25,30	26,39	34,80	50,78	21,87	30,02	54,59
19800	11,30	19,41	25,18	26,27	34,68	50,70	21,75	29,89	54,52
19900	11,22	19,29	25,06	26,14	34,56	50,61	21,63	29,77	54,45
20000	11,14	19,18	24,94	26,02	34,44	50,53	21,52	29,65	54,38

14.4 Details on numerical model

I have not made this a part of my work, but I have provided this reference from (Tang, et al., 2009):

2 NUMERICAL MODEL

In the numerical model, in order to reflect the heterogeneity of rock, the sample will be numerically discretized to many mesoscopic square elements with same size, and the thermal parameters of these elements are assumed to conform to Weibull distribution, and can be given by

$$f(\lambda) = \frac{m}{\lambda_0} \left(\frac{\lambda}{\lambda_0} \right)^{m-1} e^{-\left(\frac{\lambda}{\lambda_0} \right)^m} \quad (1)$$

where λ is the thermal conductivity of elements, λ_0 is the mean value of the element parameter and m is the shape parameter. The shape parameter m is defined as the homogeneity index of rock.

The Weibull distribution of parameter λ is given in Fig.1. It can be found that the higher the index value, m , the more homogeneous of the material. Thus, the parameter m in Eq. (1) reflects the heterogeneity of rock.

It should be noted that the discretized square elements also acted as elements for finite element analysis in the numerical model.

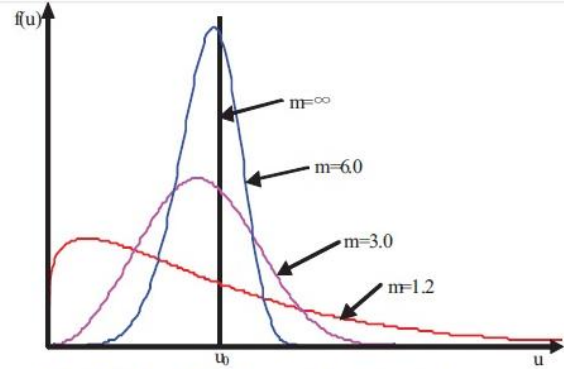


Fig. 1 Weibull distribution with different m index

According to Fourier's Law, the amount of heat to be transferred through any boundary surface can be given by

$$Q = -\lambda A \nabla^2 T \quad (2)$$

where Q is heat transfer through area A , A denotes the selected area of the surface, T represents temperature.

It can be seen from Eq. (2) that the effective thermal conductivity can be obtained as the parameters Q , A and temperature gradient are known. In this paper, the numerical thermal conductivity measurement device is shown in Fig.2. This numerical measurement device comprised a finite element grid with two perfectly insulated on the left and right sides and two sides held at constant temperature, T_1 and T_2 , respectively. Herein, it

The steady-state thermal conduction within the numerical model is governed by Laplace's Equation

$$\lambda \nabla^2 T = 0 \quad (3)$$

The relevant boundary conditions of the numerical model are

$$-\lambda \left. \frac{\partial T}{\partial x} \right|_{x=0} = -\lambda \left. \frac{\partial T}{\partial x} \right|_{x=X} = 0 \quad (4)$$

$$T|_{y=0} = T_1 \quad T|_{y=Y} = T_2 \quad (5)$$

Once finite element analysis was performed, the temperature distribution over the model was known and so it is possible to perform energy balances over the body. It is known that under the steady state thermal conduction, effective thermal conductivity can be obtained as

$$\lambda = \frac{QY}{X(T_2 - T_1)} \quad (6)$$

To invalidate the proposed numerical model and to study the influence of heterogeneity on effective thermal conductivity of rock, three groups of specimens are numerically tested. The first group is used to simulate three numerical models, i.e. serial, parallel and disordered model, to invalidate the numerical model. The second group is used to investigate the effect of heterogeneity on effective thermal conductivity.

Five specimens with different heterogeneity indices of $m = 1.2, 3.0, 6.0, 10.0$ and 30.0 represent the specimens ranging from relatively heterogeneous to homogeneous material, respectively.

The third group compares three numerically obtained effective thermal conductivity with same geometry, finite element grid and heterogeneity index, which is used to investigate the stability of numerical model.

Table 1: Homogeneity index and porosity of the specimens

	Specimen name	Homogeneity index, m
Group I	Sp#1-1 — Sp#1-3	1000
	Sp#2-1	1.2
	Sp#2-2	3.0
Group II	Sp#2-3	6.0
	Sp#2-4	10.0
	Sp#2-5	30.0
Group III	Sp#3-9 — Sp#3-11	3.0

The width of each specimen, X , is set to 100mm, and height, Y , is 200mm. The size of each element is $1 \times 1 \text{mm}^2$ throughout this paper. T_1 is set to 0°C and T_2 is 100°C . The names of these specimens are listed in Table 1.

Figure 13: Numerical model (Tang, et al., 2009).